Available online at www.sciencedirect.com
SCIENCE DIRECT®
Journal of Chromatography A, 1053 (2004) 119–131
JOURNAL OF CHROMATOGRAPHY A
www.elsevier.com/locate/chroma

Novel urea-linked cinchona-calixarene hybrid-type receptors for efficient chromatographic enantiomer separation of carbamate-protected cyclic amino acids

Karl Heinz Krawinkler, Norbert M. Maier*, Elisabeth Sajovic, Wolfgang Lindner

Institute of Analytical Chemistry, University of Vienna, Währingerstrasse 38, A-1090 Vienna, Austria

Available online 21 August 2004

Abstract

Two novel diastereomeric cinchona-calixarene hybrid-type receptors (SOs) were synthesized by inter-linking 9-amino(9-deoxy)-quinine (AQN)/9-amino(9-deoxy)-epiquinine (eAQN) and a calix[4]arene scaffold via an urea functional unit. Silica-supported chiral stationary phases (CSPs) derived from these SOs revealed, for *N*-protected amino acids, complementary chiral recognition profiles in terms of elution order and substrate specificity. The AQN-derived CSP showed narrow-scoped enantioselectivity for open-chained amino acids bearing π-acidic aromatic protecting groups, preferentially binding the (*S*)-enantiomers. In contrast, the eAQN congener exhibited broad chiral recognition capacity for open-chained as well as cyclic amino acids, and preferential binding of the (*R*)-enantiomers. Exceedingly strong retention due to non-enantioselective hydrophobic analyte–calixarene interactions observed with hydro-organic mobile phases could be largely suppressed with organic mobile phases containing small amounts of acetic acid as acidic modifier. With the eAQN-calixarene hybrid-type CSP particularly high levels of enantioselectivity could be achieved for *tert*-butoxycarbonyl (Boc)-, benzyloxycarbonyl (Z)- and fluorenylmethoxycarbonyl (Fmoc)-protected cyclic amino acids using chloroform as mobile phase, e.g. an enantioselectivty factor $\alpha > 5.0$ for Boc-proline. Increasing amounts of acetic acid compromised enantioselectivity, indicating the crucial contributions of hydrogen bonding to chiral recognition. Comparison of the performance characteristics of the urea-linked eAQN-calixarene hybrid-type CSP with those of structurally closely related mutants provided evidence for the active involvement of the urea and calixarene units in the chiral recognition process. The urea linker motif was shown to contribute to analyte binding via multiple hydrogen bonding interactions, while the calixarene module is believed to support stereodiscrimination by enhancing the shape complementarity of the SO binding site.

Keywords: Chiral stationary phases; Enantiomer separation; Urea-linked cinchona-calixarene hybrid-type selector; Cyclic amino acids

1. Introduction

Enantiomerically pure chiral cyclic amino acids represent an important class of intermediates in pharmaceutical and academic research. Their well-defined steric demands and enhanced conformational rigidity make them versatile scaffolds for drug development programs [1,2], design of efficient chiral auxiliaries and ligands for asymmetric synthesis and catalysis [3–5]. Generally, enantiomerically pure cyclic amino acids are produced by asymmetric synthesis [6] or biotransformation protocols [2]. Although these approaches have reached high levels of maturity, both can require multi-step processing, expensive reagents, catalysts, toxic metal additives and sophisticated equipment. Considering the costs and the rather long development times associated with biotransformation and asymmetric synthesis processes, chromatographic separation of the more easily accessible racemic mixtures on enantioselective chiral stationary phases (CSPs) may offer an attractive alternative [7]. Speed, scalability, short development times, the availability of continuous process technology, and straightforward access to both enantiomers in high yield and enantiomer purity are strong arguments in favor of chromatographic enantiomer separation [8,9]. However, economic preparative-scale chromatographic enantiomer separation requires readily accessible

* Corresponding author. Tel.: +43 1 4277 52373; fax: +43 1 4277 9523.
E-mail address: norbert.maier@univie.ac.at (N.M. Maier).

0021-9673/$ – see front matter © 2004 Elsevier B.V. All rights reserved.
doi:10.1016/j.chroma.2004.07.046

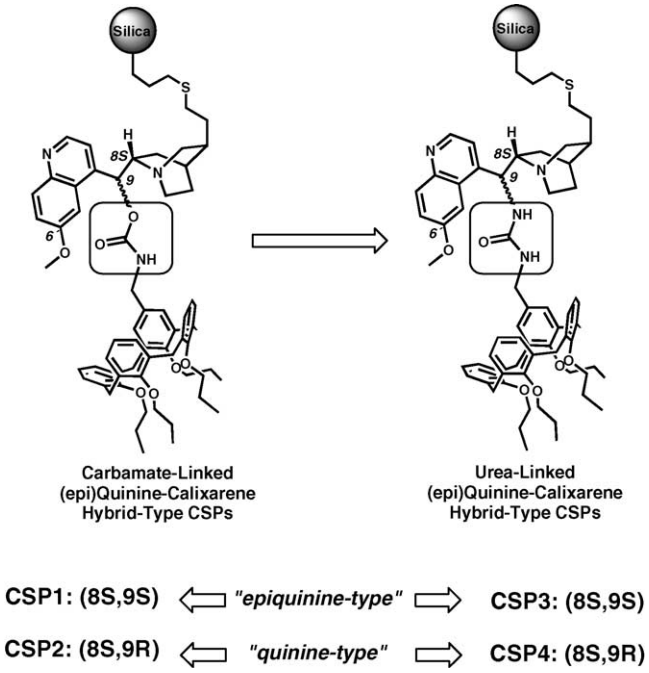

Fig. 1. Chemical structures of carbamate-linked CSP1 and CSP2, and urea-linked cinchona-calixarene hybrid-type CSP3 and CSP4.

enantioselective receptor systems (SOs) which feature high target-specific enantioselectivity, high loading capacity and broad solvent compatibility [8,9].

Addressing these needs, we have recently initiated a research program aimed at the development of dedicated cinchona-based enantioselective receptors for N-acylated cyclic amino acids, focusing on synthetically relevant carbamate-protected derivatives. In the framework of this project, two novel cinchona-calixarene hybrid-type CSPs were designed and synthesized by attaching a basket-shaped calix[4]arene module to quinine (QN) and C9-epiquinine (eQN) via a carbamate linkage (Fig. 1, CSP1 and CSP2) [10]. Integration of the calixarene module in close proximity to the cinchona unit was anticipated to assist in chiral discrimination of cyclic amino acids, either directly by specific (inclusion-type) interactions and/or indirectly by enhancement of SO shape-complementarity. Chromatographic evaluation of these C9-epimeric hybrid-type CSPs revealed complementary chiral recognition profiles for N-protected amino acids in terms of elution order, substrate specificity and solvent compatibility. The eQN-derived CSP1 exhibited preferentially enantioselectivity for N-acylated cyclic amino acids with stronger binding of the (*R*)-enantiomers, and improved chiral recognition properties in relatively apolar mobile phase environments. The QN-derived CSP2 showed preferential binding for (*S*)-enantiomers of open-chained amino acids and enhanced enantioselectivity in polar protic organic mobile phases. However, the observed levels of enantioselectivity were rather modest. Comparison of the enantiomer separation characteristics of these hybrid-type CSPs with those of the corresponding *tert*-butyl congeners revealed that the incorporated calixarene module induced anti-cooperative, rather than cooperative stereodiscriminative effects.

These disappointing results prompted us to rework and improve the original design of the cinchona-calixarene hybrid-type SOs. We reasoned that the rather flexible carbamate linker might be a source of unfavorable inter-module mobility and thus poor binding site pre-organization, prohibiting significant levels of cooperative action between the cinchona and calixarene units in enantioselective binding. To tackle this problem we decided to replace the carbamate function in CSP1 and CSP2 by a conformationally more rigid urea linker. It was anticipated that the “stiffening” effect of the urea motif [11,12] may (partially) freeze the unfavorable overall flexibility of the calixarene-cinchona assembly, and thereby induce spatially better defined and readily accessible binding domains with improved analyte shape complementarity. Apart from this binding-site shaping role, the urea linkage was hoped to provide additional opportunities for intermolecular hydrogen bonding, supporting enantioselective analyte binding.

In this paper we describe the synthesis and chromatographic evaluation of novel urea-linked cinchona-calixarene hybrid-type CSPs (CSP3 and CSP4, see Fig. 1), being derived from 9-amino(9-deoxy)-quinine (AQN) and 9-amino(9-deoxy)-epiquinine (eAQN). The crucial impact of the C8/C9-stereochemistry of the SOs integrated in these “C9-epimeric” CSPs on the overall enantiomer separation characteristics for N-protected cyclic/acyclic amino acids is demonstrated. The chiral recognition capacity of the more versatile eAQN-derived CSP3 is systematically probed in mobile phase environments with complementary solvation properties. The observed changes in enantioselectivity and retention behavior are utilized to identify specific intermolecular interaction forces contributing to chiral recognition. The relative importance of the calixarene and urea modules integrated in CSP3 to enantioselective binding of carbamate-protected cyclic amino acids is assessed by comparison of performance characteristics with those of mutant-type CSPs, comprising structurally closely related SOs lacking those functionalities.

2. Experimental

2.1. Materials

AQN and eAQN were synthesized from eQN and QN, respectively, following previously published Mitsunobu-type protocols [13,14]. 5-Isocyanatomethyl-25,26,27,28-tetrapropoxy-calix[4]arene (CalixNCO) was prepared from the corresponding amino compound as described previously [10]. Mercaptopropyl-functionalized silica gel with an SH-grafting level of 850 μmol/g was prepared from Kromasil 100 Å–5 μm (EKA Nobel, Bohus, Sweden) following the procedure reported in [15]. Dibutyltin dilaurate (95%) was purchased from Aldrich (Vienna, Austria). α,α′-Azoisobutyronitrile (AIBN) was purchased from Merck

(Darmstadt, Germany). Acetic acid (AcOH) was from J.T. Baker (Deventer, The Netherlands). All chemicals were of reagent grade and were used without any further purification. The chiral test compounds were provided by various suppliers (Aldrich, Sigma, Bachem and Degussa). Non-commercial N-acylated amino acids were synthesized following standard derivatization procedures.

2.2. General

^{1}H NMR spectra were acquired on a Bruker DRX 400 MHz spectrometer. The chemical shifts of the protons are given in parts per million (δ ppm) with respect to tetramethylsilane as internal standard. IR spectra were acquired on a Perkin-Elmer Spectrum 2000 spectrometer. Mass spectra were acquired on a PESciex API 365 triple quadrupole instrument (PESciex, Thornhill, Canada) using electrospray ionization; sample solutions in appropriate solvents were infused at concentrations of approximately 0.1 mg/ml via syringe pump (Harvard Apparatus, SO. Natick, USA) at a flow rate of 5 μl/min. The electrospray voltage was typically set to 5250 V. All reactions were carried out in oven-dried glassware under strictly anhydrous conditions and under nitrogen atmosphere. The solvents used for synthesis procedure were of purum quality and dried by standard procedures and distilled prior to use. Column chromatography was performed on silica gel purchased from Merck (0.040–0.063 mm, 230–400 mesh).

2.3. Synthesis

2.3.1. Receptors AQN-CalixU and eAQN-CalixU

To AQN (530 mg, 1.64 mmol) or eAQN (688 mg, 2.13 mmol) in 15 ml toluene, 1.2 eq. of CalixNCO [10] were added. The reaction mixture was refluxed for 17 h. The solvent was removed under reduced pressure and the residue was purified by column chromatography [50 g silica, gradient elution with $CHCl_3$–MeOH (20:1, v/v) to (10:1, v/v)].

Receptor AQN-CalixU: Yield: 500 mg (71%) of a yellowish solid. ^{1}H NMR {[$^2H_6$] dimethyl sulfoxide (DMSO-d_6)} δ: 8.66 (d, 1H); 7.88 (d, 1H); 7.75 (d, 1H); 7.44 (dd, 1H); 7.33 (dd, 1H); 6.76–6.51 (m, 5H); 6.41–6.37 (m, 4H); 6.28 (t, 1H); 6.20 (m, 1H); 6.04–5.95 (m, 2H); 5.55 (t, 1H); 5.06 (m, 2H); 4.36–4.25 (m, 4H); 3.97 (m, 2H); 3.86–3.77 (m, 7H); 3.71 (m, 4H); 3.16–3.11 (m, 3H); 3.01 (d, 1H); 2.89 (m, 2H); 2.77 (m, 1H), 2.62 (m, 1H); 2.35 (m, 1H); 2.22 (s, 1H); 1.95 (m, 1H); 1.91–1.79 (m, 8H); 1.75–1.42 (m, 4H) and 1.02–0.91 ppm (m, 12H). IR (film): ν (cm^{-1}) = 3739, 3398, 2931, 1627, 1553, 1460, 1383. MS (ESI): 971.7 $[M + H]^+$, 993.7 $[M + Na]^+$; 970 $[M - H]^-$; 1030 $[M + CH_3COO]^-$.

Receptor eAQN-CalixU: Yield: 510 mg (73%) of an off-white solid. ^{1}H NMR (C^2HCl_3) δ: 8.74 (d, 1H); 8.02 (d, 1H); 7.73 (d, 1H); 7.39 (d, 1H); 7.36 (d, 1H); 6.7–6.5 (m, 9H); 6.35 (s, 1H); 6.27 (d, 2H); 5.70 (m, 1H); 5.30 (s, 1H); 5.00 (m, 2H); 4.45–4.37 (m, 4H); 4.31 (s, 1H); 3.95 (s, 3H); 3.88–3.84 (m, 6H); 3.77 (q, 4H); 3.34–3.23 (m, 3H); 3.13 (d, 2H); 3.04 (q, 2H); 2.77 (m, 2H,); 2.35 (m, 1H); 1.96–1.85 (m, 8H); 1.73–1.46 (m, 4H); 1.03–0.94 (m, 12H) and 0.87 ppm (m, 1H). MS (ESI): 971.8 $[M + H]^+$, 993.7 $[M + Na]^+$. IR (film): ν (cm^{-1}) = 3736, 3304, 2931, 2360, 1667, 1621, 1509, 1455, 1384.

2.4. Preparation of CSP3 and CSP4

CSP3 and CSP4 were prepared according to the following general procedure: a 3.0 g amount of 3-mercaptopropyl-modified silica gel was suspended in $CHCl_3$ (20 ml) and a solution of the respective receptor (eAQN-CalixU: 686 mg, 0.70 mmol; AQN-CalixU: 880 mg, 0.90 mmol) in 10 ml $CHCl_3$ was added. After addition of AIBN (40 mg, 0.24 mmol) in $CHCl_3$ (10 ml) the suspension was refluxed for 24 h with mechanical stirring. The modified silica gel was isolated by filtration and washed with $CHCl_3$ (2 × 50 ml) and methanol (4 × 50 ml). The still wet material was re-suspended in $CHCl_3$ (40 ml) and refluxed with 1-hexene (5 ml) and AIBN (40 mg) with mechanical stirring for 7 h to deactivate residual thiol-groups. The end-capped material was isolated by filtration, washed with $CHCl_3$ (3 × 50 ml) and dried at 70 °C in high vacuum. The SO loading levels of the modified silica gels were calculated based on the nitrogen content determined by elemental analysis: CSP3: (C 15.71%; H 2.16%; N 0.89%; S 2.40%), 159 μmol/g; CSP4: (C 15.32%; H 2.13%; N 0.90%; S 2.41%), 160 μmol/g.

2.4.1. CSP1, CSPs5–7

CSP1 and CSP6 were available from prior studies [10,16]. CSP5 and CSP7 were prepared as described above by immobilization of the corresponding urea and amide-type receptors onto 3-mercaptoproply-functionalized silica gel [17]. The SO loading levels of these CSPs were as follows: CSP1: 181 μmol/g; CSP6: 290 μmol/g; CSP5: 260 μmol/g; CSP7: 245 μmol/g.

2.5. Chromatography

Chromatographic measurements were performed with a Merck-Hitachi L-7000 HPLC system (Merck, Germany), consisting of a L-7150 pump, a L-7250 programmable autosampler, a L-7455 diode array detector and a D-7000 interface. The pH-value of mobile phases (apparent pH, pH_a) was measured with an Aigner-Unilab pH meter, Model 540 GLP (Laborfachhandel, Austria). Mobile phases employed for CSP screening were composed from HPLC grade solvents (chloroform, methanol, acetonitrile) purchased from Merck.

CSP1 and CSPs3–7 were slurry packed into stainless steel columns (150 mm × 4.0 mm i.d.) by Forschungszentrum Seibersdorf (Austria) and tested under reversed phase as well as polar organic mobile phase conditions. Screening under reversed-phase conditions was carried out with a mobile phase consisting of methanol–0.1 M aqueous ammonium acetate (80:20, v/v) adjusted to pH_a 6.0 with acetic acid. The chromatographic tests in organic polar mode

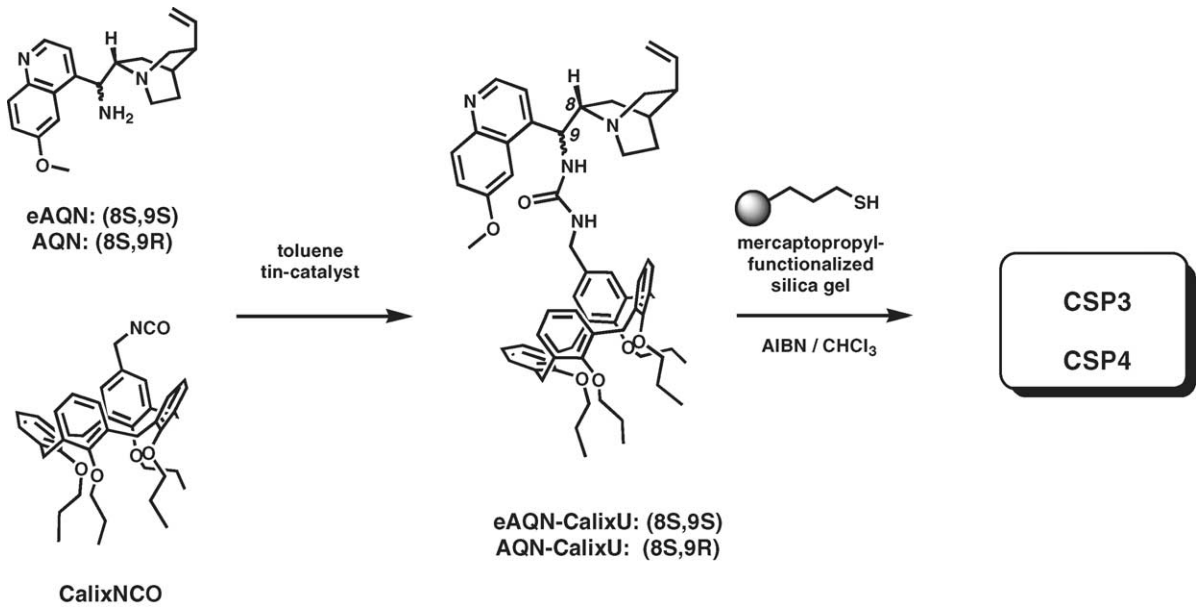

Fig. 2. Synthesis of urea-linked cinchona-calixarene hybrid-type CSP3 and CSP4.

were performed with methanol, acetonitrile and chloroform, respectively, containing 0.1–5.0% (v/v) acetic acid as an acidic modifier. Flow rate was 1 ml/min and column temperature was maintained at 25 ± 0.1 °C employing an electronically controlled thermostat. Peak detection was achieved at 254 nm for fluorenylmethoxycarbonyl (Fmoc)- and 230 nm for *tert*-butoxycarbonyl (Boc)- and benzyloxycarbonyl (Z)-derivatives. Ten-microlitre volumes of the sample solutions comprising 1 mg analyte/ml were injected.

3. Results and discussion

3.1. Synthetic aspects

The synthesis of eAQN-CalixU and AQN-CalixU, and the corresponding CSP3 and CSP4, is outlined in Fig. 2. AQN and eAQN were prepared from eQN and QN according to known Mitsunobu protocols, employing hydrazoic acid as a nucleophile, followed by Staudinger reduction [13,14]. The calixarene intermediate CalixNCO was generated by treatment of the corresponding amino precurser with diphosgen [10]. Reaction of AQN and eAQN, respectively, with CalixNCO in toluene in presence of a dibutyltin dilaurate as a catalyst gave eAQN-CalixU and AQN-CalixU in 73% and 71% yield after chromatography. Immobilization onto mercaptopropyl-modified silica gel under free radical addition conditions [16] afforded the corresponding CSP3 and CSP4 with surface loading level of 159 and 160 μmol SO/g, respectively.

3.2. Evaluation of CSPs

3.2.1. Selection of analytes

For characterization of chiral recognition profile of the CSP1 and CSPs3–7, a representative set of N-protected amino acids was employed (see Fig. 4). To sample the "substrate-specificity" of the new urea-type SOs, amino acids exhibiting different levels of steric bulkiness, hydrophobicity and polarizability were selected. The set included the open-chained amino acids alanine (Ala) and leucine (Leu) as well as *tert*-leucine (Tle), possessing sterically rather demanding aliphatic moiety, and phenylalanine (Phe), possessing an aromatic side chain. To probe the specific chiral recognition properties for cyclic amino acids, proline (Pro) and its homologues, azetidine-2-carboxylic acid (Aze) and pipecolic acid (Pipe), were evaluated. As N-protecting groups the synthetically most relevant carbamate-type protecting groups, i.e. benzyloxycarbonyl, *tert*-butoxycarbonyl and fluorenylmethoxycarbonyl were investigated. The benzoyl (Bz), 3,5-dinitrobenzyloxycarbonyl (DNZ), and the strongly π-acidic 3,5-dinitrobenzoyl (DNB) derivatives were studied as mechanistic probes, rather than for practical relevance.

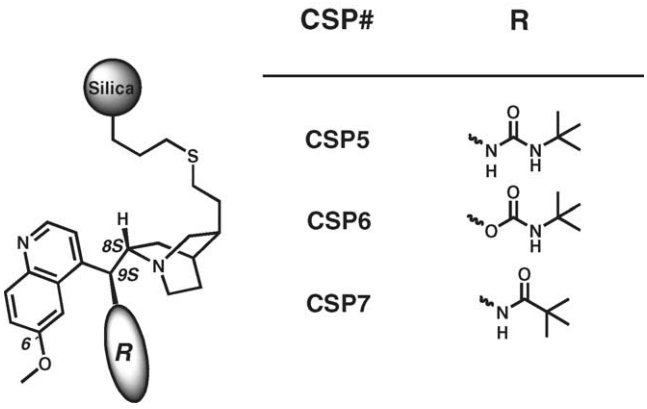

Fig. 3. Chemical structures of mutant-type CSPs5–7 structurally related to the urea-linked cinchona-calixarene hybrid-type CSP3.

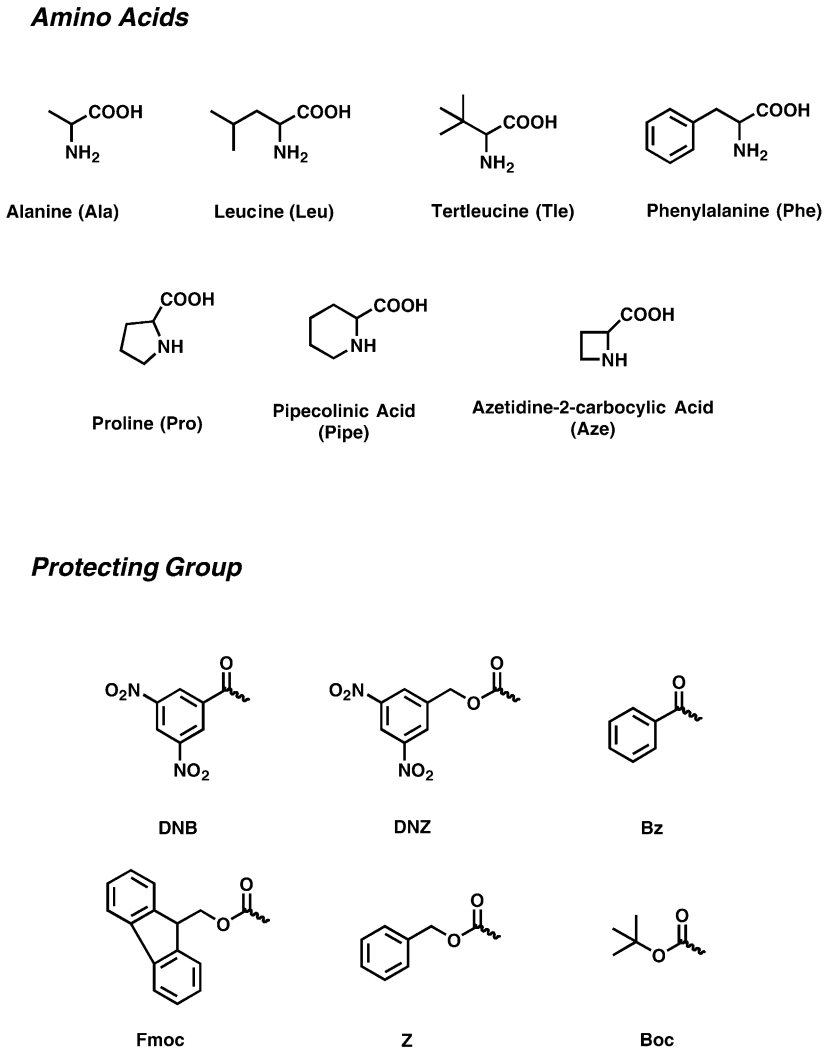

Fig. 4. Amino acids used as test analytes for the CSP evaluation and protecting groups employed for N-acylation.

3.2.2. Selection of mobile phases

Systematic chromatographic probing of SOs in mobile phases with distinct solvation properties can provide useful insights into the underlying enantioselective retention mechanisms [18,19]. On exposure to mobile phases with complementary solvation properties, the overall efficiency of enantioselective SO–analyte binding will be perturbed to different extents due to specific competing solvent–analyte and solvent–SO–analyte interactions, inducing macroscopically observable changes in the chiral recognition profile. Interpretation of these solvent-induced changes in enantioselectivity and/or retention may allow identification of the chemical nature and the specific function of molecular interaction increments contributing to chiral recognition. To take advantage of this concept, the enantiomer separation capabilities of CSP3 and CSP4 were evaluated in mobile phases with complementary solvation properties. Thus, for the initial round of screening, reversed-phase conditions (methanol–0.1 M aqueous ammonium acetate, 80:20, v/v, pH_a = 6.0, adjusted with acetic acid) were employed as mobile phase.

Further screening experiments with CSP3 were performed with buffer-free mobile phases, consisting of methanol–water (80:20, v/v), methanol, acetonitrile and chloroform, all containing 2.0% (v/v) acetic acid as an acidic mobile phase modifier. This set of solvents was anticipated to cover mobile phase environments with a broad range of polarities and specific molecular interaction qualities. Methanol–water and methanol, respectively, were selected as polar protic media with pronounced hydrogen bond donor/acceptor potential. These high-polarity media were expected to compete preferentially with electrostatic SO–analyte interactions and to specifically attack intermolecular hydrogen bonds, while enhancing hydrophobic (or solvophobic) binding increments. Acetonitrile as an aprotic strongly dipolar solvent was also anticipated to weaken electrostatic SO–analyte binding, including π–π-interactions. However, acetonitrile should affect intermolecular hydrogen bonds to a lesser extent. Finally, chloroform was employed as a low-polarity solvent with very weak hydrogen bond donor qualities, being capable of sustaining electrostatic interactions such as ion-pairing and

Table 1
Comparison of the enantiomer separation profiles of CSP3 and CSP4 for selected N-protected amino acids under hydro-organic mobile phase conditions

Analytes	CSP3				CSP4			
	k_1	k_2	α*	e.o.**	k_1	k_2	α*	e.o.**
Z-Leu	15.06	19.01	1.26	*R*	5.36		1	
Z-Tle	12.1	14.4	1.19	*R*	5.12		1	
Z-Phe	26	29.73	1.14	*R*	9.52		1	
Z-Aze	11.3	16.22	1.43	*R*	4.54		1	
Z-Pro	13.64	20.8	1.52	*R*	4.8		1	
Z-Pipe	15.63	20.83	1.33	*R*	5.97		1	
Boc-Leu	6.82	9.49	1.39	*R*	6.53		1	
Boc-Tle	5.71	7.22	1.26	*R*	2.54		1	
Boc-Phe	12.58	14.63	1.16	*R*	4.74		1	
Boc-Aze	5.28	8.47	1.6	*R*	2.21		1	
Boc-Pro	4.99	9.65	1.93	*R*	1.94		1	
Boc-Pipe	6.02	9.02	1.5	*R*	2.46		1	
Bz-Leu	7.52	9.17	1.22	*R*	3.11	4.35	1.4	*S*
Bz-Tle	6.08	6.65	1.09	*R*	3.1	3.63	1.17	*S*
Bz-Phe	11.76	13.33	1.13	*R*	5.28	6.91	1.31	*S*
Bz-Aze	8.09	11.05	1.37	*R*	3.92		1	
Bz-Pro	11.18	14.18	1.27	*R*	4.12		1	
Bz-Pipe	8.06	9.28	1.15	*R*	4.59		1	
Fmoc-Leu	27.71	38.33	1.38	*R*	11.1	12.79	1.15	*S*
Fmoc-Tle	22.2	27.59	1.24	*R*	10.12	11.48	1.14	*S*
Fmoc-Phe	49.17	58.36	1.19	*R*	19.72	22.25	1.13	*S*
Fmoc-Aze	25.49	38.88	1.52	*R*	10.78		1	
Fmoc-Pro	29.75	50.07	1.68	*R*	11.08		1	
Fmoc-Pipe	28.91	41.52	1.44	*R*	12.41	12.91	1.04	
DNZ-Leu	15.62	18.61	1.19	*R*	6.55	9.53	1.45	*S*
DNZ-Tle	13.13	14.7	1.12	*R*	6.32	9.65	1.53	*S*
DNZ-Phe	33.68	36.89	1.1	*R*	14.49	21.6	1.49	*S*
DNZ-Aze	13.23	16	1.21	*R*	6.01		1	
DNZ-Pro	19.66	26.11	1.33	*R*	6.91		1	
DNZ-Pipe	26.25	29.09	1.11	*R*	9.15		1	
DNB-Leu	16.1	19.69	1.22	*R*	6.84	40.38	5.9	*S*
DNB-Tle	13.18	14.48	1.1	*R*	6.98	25.24	3.62	*S*
DNB-Phe	23.85		1		10.52	73.19	6.96	*S*
DNB-Aze	8.84	10.12	1.14	*R*	4.76		1	
DNB-Pro	12.18	15.17	1.25	*R*	5.18		1	
DNB-Pipe	12.91		1		6.93		1	

Chromatographic conditions: CSPs: 150 mm × 4 mm i.d.; mobile phase: methanol–0.1 M aqueous CH_3COONH_4 (80:20) (v/v), pH_a = 6.0; flow rate: 1 ml/min; UV detection: 254 and 230 nm; T = 25 °C. k_1, k_2: retention factor of the less and more retained enantiomer, respectively; α*: k_2/k_1, enantiomer separation factor; e.o.**: elution order, indicating the absolute configuration of the more strongly retained enantiomer.

hydrogen bonding, but also disrupting hydrophobic association. The presence of acetic acid, a polar protic solvent with pronounced hydrogen bond donor/acceptor capacities, certainly modifies the intrinsic solvation properties of the bulk solvents to some extent. However, its influence on the specific solvation capacity of the bulk solvents was neglected at this point due to relatively low concentrations added.

3.3. Enantiomer separation characteristic of CSP3 and CSP4 under reversed-phase conditions

Generally, cinchona-type CSPs effect enantioselective analyte retention by a mixed mode ion-pairing/reversed-phase mechanism [20]. Controlling the relative contributions of these mechanisms is most conveniently achieved with hydro-organic buffered mobile phases. For this reason, the initial screening of the C9-epimeric CSP3 and CSP4 was carried out under reversed-phase conditions. The corresponding enantiomer separation data are summarized in Table 1.

Comparison of these data reveals several specific trends for CSP3 and CSP4 in terms of retention and enantioselectivity. The eAQN-derived CSP3 showed, largely independent from the structural features of the tested analyte, exceedingly strong overall retention as compared to the corresponding AQN congener CSP4 (DNB-derivatives being an exemption). Thus, for a given analyte, the retention factor of the less strongly retained enantiomer was generally two to three times higher with CSP3 than with CSP4.

This substantial difference in binding affinity cannot be rationalized based on variations in binding site density, as both CSPs possess practically identical SO loading levels (159 μmol SO/g versus 160 μmol SO/g). The epimeric SOs

in CSP3 and CSP4 are composed from identical subunits, being expected to possess quite similar solvent-exposed surface areas. Hence, dramatically different levels of hydrophobic analyte binding are also unlikely for CSP3 and CSP4.

The pronounced differences observed in analyte retention for CSP3 and CSP4 may, however, originate from different levels of binding site accessibility in the corresponding SOs. Studies on the conformational preferences of cinchona alkaloids revealed that QN and eQN, and their C9-modified derivatives, adopt, in singly protonated state, distinct low-energy conformations [21,22]. Protonated quinine exists almost exclusively in an *anti-open* conformation, aligning C9-substituents in a way to form a compact cleft-like arrangement with the quinoline [22]. On the contrary, in protonated eQN, C9-substituents prefer the opposite orientation [21], resulting in a rather extended alignment of C9-substituents relative to the quinoline group. Recent studies with amide derivatives of 9-amino(9-deoxy)epicinchonine suggest that similar conformational preferences may also exist for eAQN and AQN-derived cinchona derivatives [23].

For the AQN-derived SO in CSP4, adopting its preferred conformational state may force the extremely sterically demanding urea-linked calixarene into close proximity to the charged quinuclidinium nitrogen, being the primary interaction site for electrostatic analyte binding. Naturally, the partial occlusion of this crucial SO region may severely hamper ion-pairing interactions with approaching analytes and thus diminish overall analyte binding. More efficient electrostatic binding should be possible with the eAQN congener incorporated in CSP3, where an extended alignment of the calixarene and cinchona modules offers incoming analytes a much less hindered access to the well-exposed electrostatic interaction site.

Other important differences between the CSP3 and CSP4 exist concerning substrate specificity and preference of enantioselective binding (see Table 1). CSP3 displayed significantly more versatile chiral recognition properties than CSP4. In fact, the eAQN-derived CSP3 exhibited enantioselectivity for almost the entire set of tested analytes. In particular, CSP3 displayed efficient chiral recognition capacity for cyclic amino acids, with enantioselectivity factors up to α = 1.9. Interestingly, the nature of the N-protecting group in the analytes had a rather negligible influence on enantioselectivity.

The enantiomer separation capacity of CSP4 appeared to be restricted to open-chained amino acids (Leu, Tle and Phe) bearing Bz, Fmoc, DNZ and DNB-type N-protecting groups. The presence of the strongly π-acidic N-protecting groups, such as DNB, induced high levels of enantioselectivity (α-values up to 6.90), indicating that in these cases intermolecular $\pi-\pi$-interactions contribute favorably to the chiral recognition process.

Opposite enantiomer elution orders were observed with CSP3 and CSP4 for the limited number of analytes that could be resolved on both phases. The eAQN-derived CSP3 showed preferential binding of (*R*)-enantiomers, while its AQN congener CSP4 exhibited higher affinity to (*S*)-enantiomers. These distinct chiral recognition profiles of CSP3 and CSP4 in terms of retention characteristics, substrate specificity and enantiomer elution order are indicative of the presence of different types of chiral recognition mechanisms.

Interestingly, concerning elution order for N-acylated amino acids, the newly designed urea-linked CSP3 and CSP4 parallel the behaviors of the recently reported carbamate congeners CSP1 and CSP2 [10]. It should be pointed out that the SOs incorporated in CSP1/CSP3 and CSP2/CSP4 differ in their C9-functionalities, but possess identical C8/C9-stereochemistries (see Fig. 1). Thus, the preferential enantioselective binding for these cinchona-derived SOs appears to be dictated by the (C8,C9) stereochemistry, defining the spatial organization and the accessibility of interaction sites in the immediate proximity of the primary electrostatic binding center, rather than by the chemical nature of the remote C9-substituents. This finding is consistent with the preferential enantiomer binding observed for C9-epimeric cinchona *tert*-butylcarbamate type SOs [16].

3.4. Performance characteristics of CSP3 in mobile phases with complementary solvation properties

In view of the poor enantiomer separation capabilities of CSP4 for cyclic amino acids, further investigation concentrated on the more promising eAQN-derived CSP3. As pointed out above, screening of a given CSP with mobile phases which exhibit complementary solvation properties may help characterizing the molecular interaction forces controlling selective (and nonselective) enantiomer binding. To this end, the test analytes were screened on CSP3 with mobile phases consisting of methanol–water (80:20, v/v), methanol, acetonitrile and chloroform. All of these mobile phases were modified with 2% acetic acid to facilitate analyte elution. The following discussions are based on the assumption that the small amount of acetic acid added may not change the intrinsic solvation properties of the bulk solvents significantly.

The variation of the mobile phase solvents induced rather dramatic changes in the retention behavior and enantiomer separation characteristics of CSP3, as is evident from the chromatographic data summarized in Table 2. For all investigated analytes, enantioselectivity improved with decreasing mobile phase polarity. For instance, the enantioselectivity factor of Boc-Pro, being α = 1.93 in methanol–water, was incrementally enhanced to α = 2.07 in pure methanol and to α = 2.56 in acetonitrile, but showed quite substantial improvement to α = 5.41 in chloroform.

The pronounced gains in enantioselectivity achieved on switching from highly polar protic to low-polarity mobile phase environments provide strong evidence that intermolecular hydrogen bonding plays an important role in stereodiscrimination. Obviously, methanol–water and methanol, being strongly hydrogen bonding solvents, largely disrupt these crucial binding increments due to severe competitive SO–solvent and analyte–solvents interactions, leading to

Table 2
Impact of the bulk solvent of the mobile phase on the enantioselectivity of CSP3 for selected N-protected amino acids

Analytes	Bulk solvent of the mobile phase							
	MeOH–H_2O		MeOH		ACN		$CHCl_3$	
	k_1	α	k_1	α	k_1	α	k_1	α
Z-Leu	15.06	1.26	2.41	1.31	4.05	1.36	1.64	1.79
Z-Phe	26	1.14	6.85	1.18	9.4	1.23	3.33	1.53
Z-Aze	11.3	1.43	8.78	1.47	5.86	1.65	3.67	1.82
Z-Pro	13.64	1.52	4.78	1.54	4.3	1.67	1.84	2.4
Z-Pipe	15.63	1.33	2.94	1.32	3.65	1.3	0.69	1.54
Boc-Leu	6.82	1.39	0.96	1.49	2.02	1.64	0.85	3.05
Boc-Phe	12.58	1.16	2.97	1.21	4.72	1.37	1.91	2.31
Boc-Aze	5.28	1.6	2.57	1.68	2.14	2.09	1.27	3.2
Boc-Pro	4.99	1.93	1.22	2.07	1.6	2.56	0.66	5.41
Boc-Pipe	6.02	1.5	0.91	1.46	1.65	1.44	0.4	2.28
Fmoc-Leu	27.71	1.38	3.34	1.45	5.72	1.42	1.27	2.07
Fmoc-Phe	49.17	1.19	9.8	1.22	12.74	1.28	2.73	1.57
Fmoc-Aze	25.49	1.52	13.56	1.58	8.64	1.74	2.5	2.33
Fmoc-Pro	29.75	1.68	7.63	1.75	6.41	1.9	1.21	3.37
Fmoc-Pipe	28.91	1.44	4.23	1.42	5.08	1.37	0.89	1.82
Bz-Leu	7.52	1.22	2.11	1.3	6.13	1.54	5.68	2.34
Bz-Phe	11.76	1.13	6.01	1.18	13.41	1.4	9.06	1.94
Bz-Aze	8.09	1.37	10.11	1.48	6.77	1.61	9.15	1.51
Bz-Pro	11.18	1.27	5.95	1.35	8.9	1.55	10.07	1.52
Bz-Pipe	8.06	1.15	2.92	1.18	5.62	1.25	1.78	1.37
DNZ-Leu	15.62	1.19	2.76	1.25	3.79	1.26	2.84	1.55
DNZ-Phe	33.68	1.1	7.65	1.12	8.67	1.14	5.62	1.35
DNZ-Aze	13.23	1.21	10.65	1.3	5.56	1.37	5.45	1.47
DNZ-Pro	19.66	1.33	7.5	1.39	3.74	1.52	2.13	1.94
DNZ-Pipe	26.25	1.11	4.93	1.13	3.31	1.12	0.92	1.25
DNB-Leu	16.1	1.22	4.5	1.32	8.49	1.36	23.34	1.87
DNB-Phe	23.85	1	12.86	1.09	19.1	1.21	38.14	1.6
DNB-Aze	8.84	1.14	30.84	1.2	16.49	1.34	39.03	1.51
DNB-Pro	12.18	1.25	17.25	1.31	12.77	1.49	18.73	1.96
DNB-Pipe	12.91	1	10.14	1	8.36	1.08	4.59	1.27

(a) All mobile phases contain 2% (v/v) acetic acid as a modifier. (b) MeOH–water (80:20, v/v) for chromatographic conditons see Table 1.

rather poor levels of enantioselectivity. Acetonitrile, a highly polar but rather poor hydrogen bonding solvent, supports intermolecular hydrogen bonding, and therefore improves enantioselective binding. In the weakly competing and relatively apolar chloroform environment the stability of the crucial intermolecular hydrogen bonding networks is further enhanced and, consequently, enantioselectivity maximized.

Solvent-induced changes in analyte retention observed with CSP3 exhibited an opposite trend. Particularly with analytes bearing carbamate type N-protecting groups (Boc, Z, Fmoc, DNZ), retention was dramatically diminished as mobile phase polarity was decreased. This effect was especially pronounced with analytes bearing highly lipophilic protecting groups comprising aromatic elements as can be seen from the retention data of Fmoc amino acids depicted in Fig. 5. For example, the retention factor of the less retained Fmoc-(*R*)-Aze enantiomer decreases in the order methanol–water > acetonitrile > methanol > chloroform from k_1 = 1.27–24.49 (see Fig. 4). The exceedingly strong analyte retention observed with the methanol–water mobile phase, being readily disrupted in presence of low-polarity solvents, is diagnostic of strong hydrophobic interactions between the calixarene

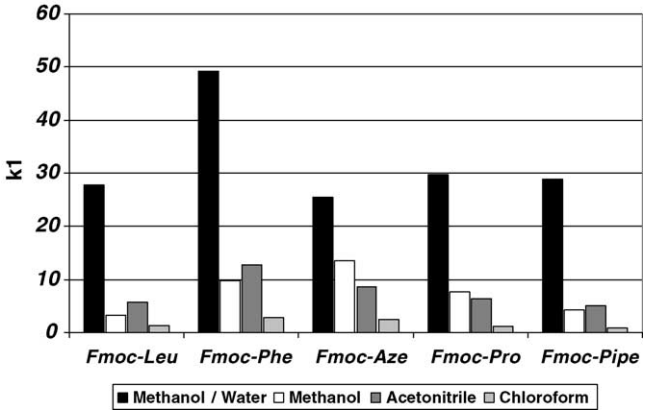

Fig. 5. Retention characteristics of the less strongly retained (*R*)-enantiomer of selected Boc amino acids on CSP3 under various mobile phase conditions. All mobile phases contain 2% (v/v) acetic acid as acidic modifier. The composition of the methanol–water is 80:20 (v/v). For chromatographic conditions see Table 1.

module in the SOs and the lipophilic structure elements of the analytes [24,25].

Analytes bearing benzoyl-type protecting groups, particularly DNB-amino acid derivatives, show a less easily interpretable retention characteristics. As can be seen from the data in Table 2, the retention behavior of these analytes deviates from that observed for carbamate-protected derivatives. For most cases, analyte retention remains at relatively high levels or even increases on switching from polar protic to low-polarity mobile phase conditions. This particular behavior may be rationalized by considering the multi-facetted molecular interaction potential of π-acidic aromatic ring systems [26]. A recent study on the stability of supermolecularly π-stacked foldamer assemblies in various solvent systems established that aromatic π–π-complex stabilization is governed primarily by hydrophobic (solvophobic) interactions, but may also involve electrostatic binding contributions [27]. Naturally, aromatic groups with extended π-systems provide large lipophilic domains which rapidly aggregate to other lipophilic surfaces by hydrophobic adhesion on exposure to polar protic media. However, placing polarizing substituents at aromatic systems induces substantial quadrupol moments [28], making them also capable of undergoing electrostatic interaction with complementary polarized groups. The strong retention of DNB-protected amino acids on CSP3 in polar as well as in apolar mobile phases probably reflects mixed-mode interactions involving hydrophobic and electrostatic aromatic interaction increments. In the methanol–water mobile phases, the strong analyte binding may primarily be caused by hydrophobic adhesion between the extended surfaces of the π-acidic DNB-group and the π-basic calixarene module. On switching to chloroform, these hydrophobic interactions may be largely suspended, but readily (over)compensated by activation of the electrostatic binding increments.

The data in Table 2 demonstrate that the strong hydrophobic interactions dominating the retention behavior of N-acylated amino acids on CSP3 in methanol–water environment are evidently non-enantioselective in nature. For carbamate-protected analytes the less favorable strong hydrophobic interactions can be conveniently disrupted with methanol, acetonitrile and in particular chloroform mobile phases, without sacrificing enantioselective binding capacity.

3.5. Influence of the acidic modifier concentration

To further advance our knowledge on the mobile phase influences effecting the chiral recognition capacity of CSP3 the impact of acidic modifier concentration on enantioselective analyte binding was studied. For this purpose, Boc-Pro was chromatographed on CSP3 with mobile phases consisting of chloroform and variable amounts of acetic acid (0.1–5.0%, v/v).

Diminishing the amount of acetic acid in the mobile phase led to a significant enhancement in analyte retention (see Fig. 6A). Plotting logarithmically the retention factors of

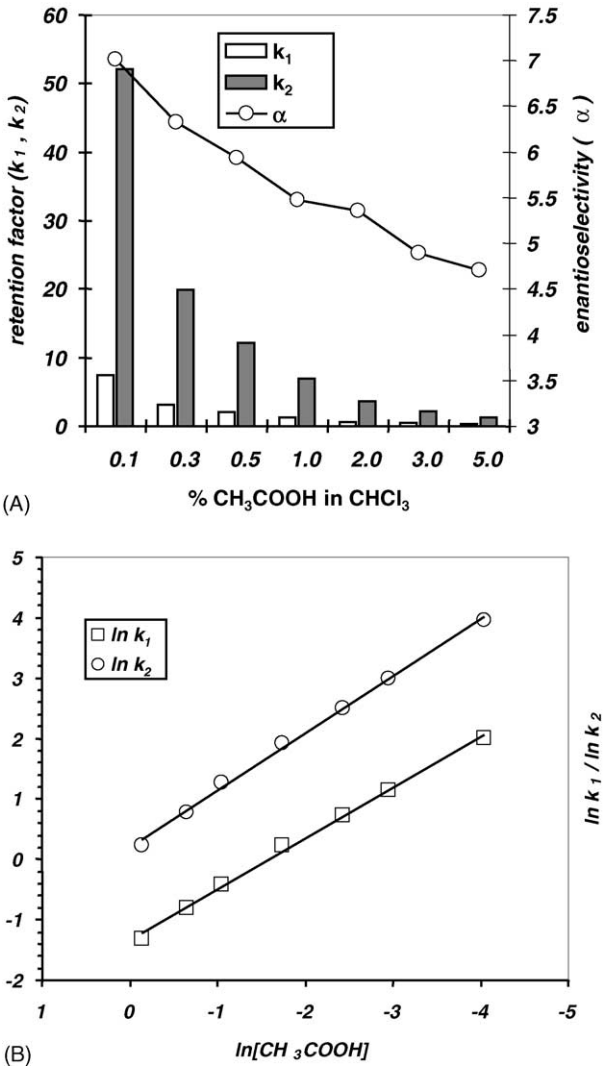

Fig. 6. (A) Dependency of retention and enantioselectivity for Boc-Pro on the acetic acid modifier concentration in chloroform. (B) Double ln-plot of the retention factors of Boc-Pro on CSP3 vs. the acetic acid modifier concentration in chloroform. The linear relationship is indicative of an anion-exchange retention mechanism. For other chromatographic conditions see Table 1.

both Boc-Pro enantiomers versus the mobile phase acetic acid concentrations produces roughly straight lines (see Fig. 6B). These linear relationships are diagnostic for the existence of an anion-exchange-type retention mechanism [29]. Thus, although poorly dissociated in chloroform, acetic acid is capable of acting as an acidic anion displacer, readily disrupting the strong electrostatic interaction existing between the oppositely charged analytes and the SO.

As is evident from Fig. 6A, diminishing the acetic acid concentration in the mobile phase also induced a significant enhancement in enantioselectivity for Boc-Pro. For instance, with 5% acetic acid, α = 4.71 was achieved, which could be increased to α = 7.01 upon lowering the acetic acid concentration to 0.1%. Even at rather low concentration levels in low-polarity mobile phases, acetic acid does impair

enantioselective SO–analyte binding. Considering the exceedingly strong hydrogen bond donor/acceptor capacity of acetic acid, competitive hydrogen bonding to crucial interaction sites of the analytes and the SO may account for this interfering mechanism.

3.6. Assessment of the contributions of the calixarene module and urea-linkage to chiral recognition

To assess the specific contributions of the urea and calixarene structure elements incorporated in CSP3 to enantioselective binding of carbamate-protected amino acids, its chiral recognition profile was compared with that of a set of *structural mutants*. These mutants, available from previous studies, comprised CSP1 (see Fig. 1) and CSPs5–7 (see Fig. 3). As a shared structural feature with CSP3, all these CSPs were derived from cinchona scaffolds exhibiting *eQN-type stereochemistry*, i.e. (8S,9S)-configuration. Apart from common stereochemistry, these mutants differ from CSP3 in following structural details: (i) CSP1: replacement of the C9-NH by an oxygen; (ii) CSP5: replacement of the calixarene module by a *tert*-butyl group; (iii) CSP6: replacement of the calixarene module by a *tert*-butyl group, plus replacement of the C9-NH by an oxygen; (iv) CSP7: combined replacement of the calixarene module and beta-NH by a *tert*-butyl group.

To generate a data set allowing a comparative analysis of the enantiomer separation performance, a limited set of carbamate-protected amino acids was screened on CSP3 and the corresponding mutant-type CSPs, employing a mobile phase consisting of chloroform modified with 0.5% acetic acid. The corresponding enantiomer separation and retention data are given in Table 3. It should be pointed out that the mutant CSPs exhibit higher SO loading levels than CSP3. These variations in binding site density may significantly affect overall retention behavior, but to a lesser extent the enantioselective binding [30]. For this reason, the following comparative analysis focuses on the enantioselectivity data only.

As can be seen from the data in Table 3, CSP3, incorporating the urea-linked eAQN-calixarene hybrid-type SO, clearly outperformed all structurally related mutant CSPs. Excellent enantioselectivity factors could be obtained for all evaluated carbamate-protected amino acids, with the enantiomers of cyclic amino acids being particularly well resolved. Boc-derivatives showed the highest levels of enantioselectivity on CSP3, with enantioselectivity factors ranging from 2.36 to 5.94.

Comparison of the chiral recognition performance of CSP3 with that of the corresponding carbamate-linked CSP1 allows estimation of the favorable increments provided by of the urea-linkage to enantioselective binding. As is evident from the data in Table 3, the carbamate/urea-linker mutation induced dramatic gains in chiral recognition capacity, with improvements in α-values by factors up to >4. It is informative to express the achieved improvements in enantioselectivity in terms of changes in differential free energy of enantioselective binding ($\Delta\Delta G = -RT\ln\alpha$). The $\Delta\Delta G$-values for Boc-amino acids on CSP3 and the corresponding mutant CSPs are depicted in Fig. 7. The replacement of the carbamate linker by a urea functions (CSP1 versus CSP3) induces gains in $\Delta\Delta G$ ranging from -1.5 to -3.5 kJ/mol. Interestingly, this gain in enantioselective binding energy is consistent with the stabilizing effects observed on the formation of a weak hydrogen bond.

The contribution of the calixarene module to enantioselective binding was established by comparing the chiral recognition properties of CSP3 and CSP5. Similar to the CSP3, mutant-type CSP5 possesses an urea linkage, but instead has

Table 3
Comparison of enantiomer separation profiles of CSP3 and mutant type CSP1 and CSPs5–7 for N-carbamate protected amino acids

Analytes	CSP3		CSP1		CSP5		CSP6		CSP7	
	k_1	α	k_1	α	k_1	α	k_1	α	k_1	α
Z-Leu	6.72	1.86	3.28	1.25	10.18	1.65	11.45	1.21	12.65	1.04
Z-Ala	15.86	1.57	7.03	1.14	22.92	1.42	25.8	1.13	24.96	1.03
Z-Phe	14.92	1.55	7.31	1.13	22.05	1.33	25.06	1.12	26.43	1.06
Z-Aze	14.37	2.07	4.89	1.2	14.04	2.11	11.71	1.35	14.79	1.38
Z-Pro	8.16	2.62	2.31	1.29	7.55	2.72	5.18	1.52	8.27	1.3
Z-Pipe	3.3	1.7	1.53	1.18	4.07	1.47	3.78	1.15	4.58	1.15
Boc-Leu	4.53	3.42	1.69	1.43	5.81	2.59	5.98	1.38	6.19	1
Boc-Ala	7.8	2.54	3.69	1.26	11.38	2.07	13.2	1.23	12.64	1
Boc-Phe	10.56	2.36	3.43	1.3	12.41	1.87	13.49	1.23	11.95	1.14
Boc-Aze	4.04	4	1.43	1.34	4.35	3.19	3.27	1.56	5.27	1.3
Boc-Pro	2.62	5.94	0.94	1.4	3.02	4.49	2	1.74	3.37	1.27
Boc-Pipe	1.97	2.62	1.96	1.18	2.64	1.83	2.2	1.26	2.72	1.13
Fmoc-Leu	5.31	2.12	2.98	1.21	9.02	1.82	9.55	1.26	9.94	1.08
Fmoc-Ala	11.81	1.7	6.28	1.17	19.39	1.49	21.76	1.11	21.16	1.06
Fmoc-Phe	12.28	1.57	6.22	1.14	19.88	1.39	21.49	1.15	20.62	1
Fmoc-Aze	10.81	2.6	4	1.22	12.69	2.31	9.1	1.38	11.12	1.44
Fmoc-Pro	4.76	3.45	1.81	1.35	6.26	3.14	3.75	1.63	5.71	1.42
Fmoc-Pipe	2.49	2.1	1.22	1.2	3.33	1.68	2.9	1.18	3.39	1.21

Mobile phase: 0.5% acetic acid in chloroform; for other conditions see Table 1.

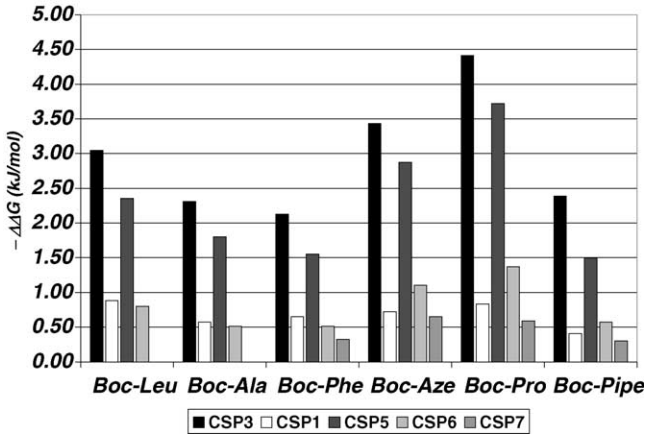

Fig. 7. Comparison of the differential free energies of enantioselective binding ($\Delta\Delta G$) for various Boc-amino acids observed on CSP3 and the corresponding mutant-type CSP1 and CSPs5–7. For chromatographic conditions see Table 3.

the sterically demanding calixarene module replaced by a significantly smaller *tert*-butyl group. Higher levels of enantioselectivity observed with CSP3 as compared to CSP5 provide conclusive proof for favorable contributions of the calixarene module to chiral recognition. The improvements in enantioselectivity associated with the *tert*-butyl/calixarene mutation (CSP5 versus CSP3), however, are relatively small compared to those found with the carbamate/urea exchange (CSP1 versus CSP3). Thus, for Boc-Pro, the replacement of the *tert*-butyl function with the calixarene module induced a modest increase from α = 4.49 to 5.94. Expressed in terms of change in differential free energy of binding, this gain corresponds to a comparably small energetic increment of −0.7 kJ/mol. These observations suggest that the highly favorable chiral recognition capabilities of CSP3 originate largely from the urea linkage, with the calixarene module making minor supportive contributions to enantioselective analyte binding.

More refined information on the crucial structural requirements of the C9-linker functionality for enhancing enantioselective binding can be obtained by comparing the enantiomer separation profiles for CSPs5–7, which provide a consistent set of linker modifications. Thus, CSPs5–7 are derived from SOs comprising an urea-, a carbamate- and an amide-linked *tert*-butyl group as C9-functionality, respectively. Consistent with the observations made for the calixarene hybrid-type CSP1 and CSP3, the replacement of the urea linker in CSP5 for a carbamate function led to a major loss in enantioselectivity, with changes in $\Delta\Delta G$ in the range of 1.0–2.0 kJ/mol. Formally, this highly unfavorable CSP6/CSP5 mutation involves the exchange of the C9-NH for an oxygen only, which should not affect the spatial requirements of the linker units dramatically. Hence, the C9-NH group in CSP5 must serve as a functional binding element in the chiral recognition process of carbamate-protected amino acids.

A comparison of the chiral recognition performance of CSP5 and CSP7, comprising an urea and an amide-type linker, respectively, reflects the severe consequences of the formal deletion of the remote NH in the urea linker unit. As can be seen from the data in Table 3 and Fig. 7, this mutation induced an even more significant drop or even a complete loss in enantioselectivity. This finding provides compelling evidence that only a fully preserved urea motif can contribute favorably to chiral discrimination.

The urea-linkage incorporated into CSP3 (and CSP5) not only functions as a passive rigidifying connector between the cinchona and calixarene modules, but also participates actively in chiral recognition. The combined evidence emerging from SO mutation experiments and the sensitivity to solvents with competing hydrogen bonding capacities, establish that the urea-linkage acts as a well-defined hydrogen bond donor motif in enantioselective analyte binding.

3.7. Mechanistic consideration

Considering the structural features of the SO in CSP3, enantioselective analyte binding may occur in a well-localized fashion at the inter-module domain, being spatially defined by the conformationally rather rigid urea linker and flanked by the cinchona and calixarene units. Analyte binding to this domain may primarily be driven by ion-pairing interaction with the protonated quinuclidine nitrogen, with stereodiscrimination resulting from shape selectivity of the binding domain and formation of supportive intermolecular hydrogen bond networks. The importance of shape complementarity is nicely reflected by the enantiomer separation characteristics of CSP3 for conformationally rigid carbamate-protected cyclic amino acids. For these analytes, the level of enantioselective and substrate specific binding is significantly influenced by the ring size of the amino acid and the nature of the attached protecting group. As can be seen from the data in Table 3, analyte retention decreases with increasing steric demands of the cyclic amino acids, with small-sized azetidine-2-carboxylic acid derivatives being more strongly retained than larger pipecolic acid congeners. In similar fashion, analytes bearing sterically demanding and bulky protecting groups are less retained (Boc < Fmoc < Z) than those with smaller or conformationally more flexible groups.

Also, the efficiency of enantioselective binding for cyclic amino acids is influenced by the ring size and nature of the protecting groups. Most efficient chiral recognition is achieved for Pro derivatives, followed by Aze and Pipe. The size of the analytes evidently determines the degree of accessibility to the urea hydrogen bonding motif located within the binding domain defined by the inter-linked cinchona and calixarene modules. Small-sized Aze derivatives should experience little steric hindrance on approaching the urea-linkage to form hydrogen bonds. Thus, enantioselective binding may primarily involve the efficient intermolecular hydrogen bonding, resulting in relative strong retention. For the larger Pro derivatives, however, enhanced steric hindrance may compromise binding site accessibility, but more so for the less

retained enantiomer. Simultaneous occurrence of "stereoselective exclusion" for the less favorable enantiomer and efficient hydrogen bonding for the favorable enantiomer may explain the particularly efficient chiral discrimination observed with Pro-derivatives. Naturally, the partial rejection of the less favorable analyte should result in a loss in overall retention. The pronounced steric demands of the larger Pipe-derivatives may impair binding site accessibility, but for both enantiomers, resulting in diminished interaction with the urea hydrogen bond motif and a further loss in overall enantioselectivity and retention. The presence of sterically bulky protecting groups, such as Boc, is expected to assist the stereoselective exclusion phenomena outlined above, and should consequently lead to reduced retention and improved enantioselectivity. The opposite should be true for protecting groups with smaller or more flexibly tethered Fmoc and Z derivatives.

For open-chained carbamate-protected amino acid (Ala, Leu and Phe) stereoselective exclusion effects are expected to contribute less significantly to stereodiscrimination as their enhanced conformational flexibility facilitates binding site access and adaptive interaction with the urea hydrogen bond motif. More efficient hydrogen bonding in combination with poor stereoselective shape discrimination should result in increased retention and decreased enantioselectivity.

This mechanistic picture, being fully consistent with the experimental results, may be useful to guide the design of improved versions of urea-linked cinchona-type SOs. Considering the demonstrated importance of the urea motif for intermolecular hydrogen bonding, the introduction of thiourea linkers with increased hydrogen bond acidity may further enhance the enantioselective binding capabilities. Tuning shape selectivity by replacement of the calixarene module by smaller, but conformationally less flexible scaffolds may offer another promising strategy to further improvements.

4. Conclusions

Two novel diastereomeric cinchona-calixarene hybrid-type SOs were synthesized by inter-linking 9-amino(9-deoxy)-quinine/9-amino(9-deoxy)-epiquinine and a calix[4]arene scaffold via an urea function. Immobilization of these SOs onto silica and evaluation of the resultant CSPs with a set of N-protected amino acids in buffered hydro-organic mobile phases revealed complementary chiral recognition profiles in terms of elution order and substrate specificity. The AQN-derived CSP showed a narrow scope of enantioselectivity for open-chained amino acids bearing π-acidic protecting groups, preferentially binding the (*S*)-enantiomers. The eAQN congener exhibited broad chiral recognition capacity for open-chained, and particularly cyclic amino acids, and preferential binding of (*R*)-enantiomers.

Systematic screening of the more versatile eAQN derived CSP in mobile phase environments with complementary solvation properties established acetic acid-modified chloroform as an ideal mobile phase. Specifically, this mobile phase disrupted the exceedingly strong hydrophobic retention observed in hydro-organic mobile phases and dramatically enhanced enantioselectivity for carbamate-protected cyclic amino acids. Chromatographic experiments performed with variable concentrations of acetic acid in chloroform revealed retention characteristics consistent with an anion exchange mechanism. Increasing amounts of acetic acid compromised enantioselectivity, indicating the crucial contribution of hydrogen bonding interactions to chiral recognition.

Comparison of the performance characteristic of the urea-linked eAQN-calixarene hybrid-type CSP with those of structurally closely related mutants provided conclusive evidence for the active involvement of the urea and calixarene units in the chiral recognition process. The urea linker motif was shown to contribute to analyte binding via multiple hydrogen bonding, while the calixarene module enhanced shape complementarity of the binding site. Further optimization of the chiral recognition capacity of eAQN-derived urea-type SO may be possible by enhancing hydrogen bonding acidity of the urea linkage and shape complementarity of the binding domain, e.g. by introduction of thiourea motifs and replacement of the conformationally flexible calixarene module by more rigid scaffolds.

Acknowledgements

This project was supported by grants from the Austrian Research Fund (FWF) Projects Nos. P14179-CHE and P16300-B1. Our thanks to Dr. Kevin Schug for providing competent linguistic advice.

References

[1] J.S. Ma, Chim. Oggi 21 (2003) 65.
[2] M. Petersen, M. Sauter, Chimia 53 (1999) 608.
[3] E.J. Corey, C.J. Helal, Angew. Chem. Int. Ed. 37 (1998) 1986.
[4] A. Job, C.F. Janeck, W. Bettray, R. Peters, D. Enders, Tetrahedron 58 (2002) 2253.
[5] B. List, Terahedron 58 (2002) 5573.
[6] C. Cativiela, M.D. Diaz-De-Villegas, Tetrahedron: Asymmetry 11 (2000) 645.
[7] N.M. Maier, P. Franco, W. Lindner, J. Chromatogr. A 906 (2001) 3.
[8] E.R. Francotte, J. Chromatogr. A 906 (2001) 379.
[9] M. Schulte, J. Strube, J. Chromatogr. A 906 (2001) 399.
[10] K.H. Krawinkler, N.M. Maier, R. Ungaro, F. Sansone, A. Casnati, W. Lindner, Chirality 15 (2003) 17.
[11] N.M. Maier, G. Uray, J. Chromatogr. A 732 (1996) 215.
[12] F. Hettche, P. Reiss, R.W. Hoffmann, Chem. Eur. J. 8 (2002) 4946.
[13] H. Brunner, J. Buegler, B. Nuber, Tetrahedron: Asymmetry 6 (1995) 1699.
[14] H. Brunner, J. Buegler, Bull. Soc. Chim. Belg. 106 (1997) 77.
[15] E. Veigl, B. Böhs, A. Mandl, D. Krametter, W. Lindner, J. Chromatogr. A 694 (1995) 135.
[16] N.M. Maier, L. Nicoletti, M. Lämmerhofer, W. Lindner, Chirality 11 (1999) 522.

[17] N.M. Maier, E. Sajovic, W. Lindner, unpublished results.
[18] B. Chankvetadze, I. Kartozia, C. Yamamoto, Y. Okamoto, J. Pharm. Biomed. Anal. 27 (2002) 467.
[19] A. Berthod, T.L. Xiao, Y. Liu, W.S. Jenks, D.W. Armstrong, J. Chromatogr. A 995 (2002) 53.
[20] M. Lämmerhofer, N.M. Maier, W. Lindner, Am. Lab. 30 (1998) 71.
[21] G.D.H. Dijkstra, R.M. Kellogg, H. Wynberg, J.S. Svendsen, I. Marko, K.B. Sharpless, J. Am. Chem. Soc. 111 (1989) 8069.
[22] N.N. Maier, S. Schefzick, G.M. Lombardo, M. Feliz, K. Rissanen, W. Lindner, K.B. Lipkowitz, J. Am. Chem. Soc. 124 (2002) 8611.
[23] H. Brunner, P. Schmidt, M. Prommesberger, Tetrahedron: Asymmetry 11 (2000) 1501.
[24] T. Sokoliess, U. Menyes, U. Roth, T. Jira, J. Chromatogr. A 898 (2000) 35.
[25] T. Sokoliess, J. Schönherr, U. Menyes, U. Roth, T. Jira, J. Chromatogr. A 1021 (2003) 71.
[26] E.A. Meyer, R.K. Castellano, F. Diederich, Angew. Chem. Int. Ed. Engl. 42 (2003) 1210.
[27] M.S. Cubberley, B.L. Iverson, J. Am. Chem. Soc. 123 (2001) 7560.
[28] N.J. Heaton, P. Bello, B. Herradon, A.D. Campo, J. Jimenez-Barbero, J. Am. Chem. Soc. 120 (1998) 9632.
[29] J. Ståhlberg, J. Chromatogr. A 855 (1999) 3.
[30] J. Lah, N.M. Maier, W. Lindner, G. Vesnaver, J. Phys. Chem. B 105 (2001) 1670.